ULTIMATE ANALYSIS OF STRUCTURES EXPOSED TO SEISMIC EFFECTS

by

B. CSÁK

Department of Strength of Materials and Structures, Technical University, Budapest

Received: March 15th, 1978
Presented by Dr. J. PEREDY

1. Introduction

Actually, load bearing structures are designed either

— by the traditional — classic — method of elastic analysis; or

— by the plastic limit analysis, of increasing popularity.

Application of either method in actual cases depends on the design specifications in the concerned country. In general, specification of one or other method is partly defined by the purpose — importance, technological function of the construction, — and partly by the kind of expected stresses. In relation to the construction, of course no ultimate design will be allowed for a nuclear reactor or a dam or another construction where cracks or plastic deformations may induce destructive processes more hazardous from many aspects than damaging of the construction itself.

As concerns load and stresses, in case of permanent or frequent loads, it is righteous to require the structure to be exempt from plastic deformations or other changes.

This is not the case of loads or effects of low probability to occur during the planned service life of the construction.

Such an effect is earthquake — except, of course, in seismic zones.

Let us consider now the problems of designing exclusively for seismic effects as extraordinary load of low probability, with the following assumptions:

— The critical — enhanced — load case is seismic effect, namely here seismic stresses exceed those arising from any other load or effect.

— Seismic effect is considered as an extraordinary load of low probability throughout the service life of the construction.

— Rather than to house extremely important and hazardous operations, the tested constructions are average ones where no additional catastrophe arises from plastic failures — development of plastic hinges and great plastic deformations — induced by seismic effects.

Design criterion of these buildings may be safety from sudden collapse, from the risk of burying lives and values. With buildings thus damaged, it is accepted to renounce of an ulterior reconstruction or strengthening.

2. Practical observations, experience

Ulterior evaluation of a heavy earthquake normally involves the following damage categories:

— complete collapse;
— heavy structural damage; impossibility of repair;
— heavy but reparable damage;
— light damage;
— no structural damage.

Problems related to the second category will be considered from the aspects quoted in the former item.

Investigation of structural damages of buildings in this category demonstrates and permits to ulteriorly evaluate the failure mechanism of the structural system.

Of course, also analysis results of the failure mechanism in subsequent categories have to be made use of, in particular to learn the internal reserve — either fully or partly exhausted — of the structure during the development of the failure mechanism and involved in the resistance of the structure.

These tests define among others the elastic and plastic internal resistance energy of the structural system against the seismic effect representing an external energy to be learned ulteriorly.

These values can be expressed by the deformation work of the damaged structural system.

Ulterior evaluations unambiguously point to the importance of ductility in terms of the elastic to plastic deformation ratio.

According to Fig. 1, deformation works — inner resistances — of the structure in elastic and plastic condition — shaded and clear areas, resp. — differ by orders of magnitude.

This is increasingly true for the case of load or deformation cycles caused, e.g., by consecutive shock waves.

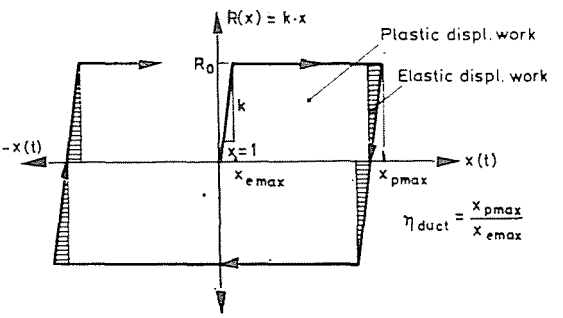

Fig. 1. Elasto-plastic displacement-resistance diagram

Fig. 1 contains deformation $x(t)$ as an independent variable and $R(x)$ as internal resistance of the structure, with the elastic limit R_0. This is the resistance value of the structure in the plastic range.

Since the value of deformation work — potential energy — is expressed by the area below the curve, the plastic deformability x is at least as important as the peak resistance R_0.

Details of a failure mechanism where great plastic deformations could develop without structural collapse and decomposition have been published in [4].

In this case the deformation was throughout accompanied by resistance — potential energy — able to absorb — dissipate — the external energy. Thus, throughout the motion, the basic equation expressing the equality of energy maxima was satisfied:

$$E_{\text{kin max}} = E_{\text{pot max}}$$

where $E_{\text{kin max}}$ is seizmic motion energy, and $E_{\text{pot max}}$ the structural resistance energy maxima of external and internal work, respectively.

On the other hand, cases seen in Fig. 2 and [19] are those of disjointing due to missing ductility. Here deformations involve no resistance any more and the structure remains undamped until failure.

Rather than by disconnections alone, structures may fully or partly collapse by stability loss of structural members.

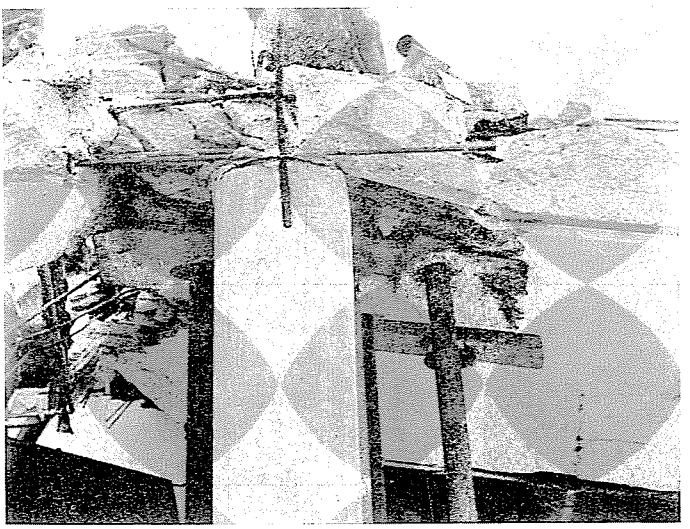

Fig. 2

Integer motion of the entire structure is thus primordial to prevent deformation especially of axially loaded members likely to induce stability loss.

Failure by stability loss is seen in Fig. 3.

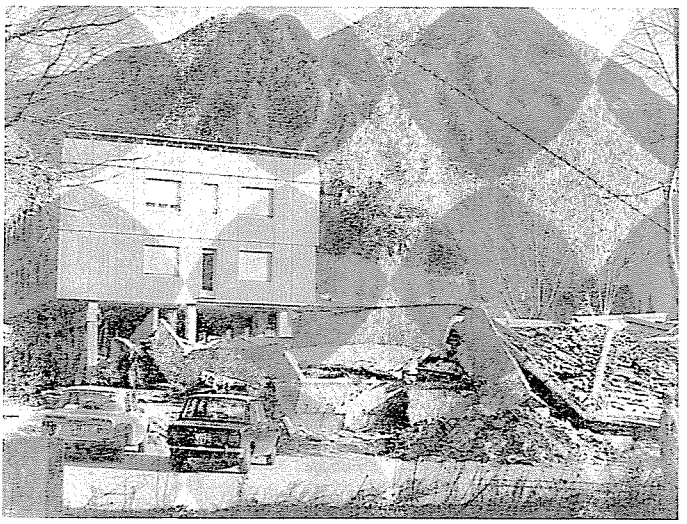

Fig. 3

The following conclusions can be drawn:

Examination of the failure mechanism shows plastic hinges to develop in the structural system. If their location is such as not to cause stability loss of other members, and the plastic hinges still possess some ductility, the structure, though heavily damaged, does not collapse. Otherwise the structure collapses either by stability loss or by ductility exhaustion.

These considerations rise two essential problems:

— How to construct a structure so as to develop plastic hinges in places possibly favourable for the energy absorptiveness of the structure, hence for an optimum structural resistance, and not to induce stability loss of other structural members?

— How to design plastic hinges — especially in reinforced concrete structures — to keep an adequate plastic deformability — ductility — even after cyclic deformations?

3. Conditions and possibilities of plastic analysis

3.1 Conditions

The conditions of admitting deformations and other alterations concomitant to the plastic range depend on the expected seismic behaviour of the construction.

In every country, this problem is controlled by relevant chapters of the seismic design specifications in virtue.

3.2 Possibilities

Possibilities essentially arise from the effect of alternating, abrupt shock-like, pulse-like loads on the structure.

In an earthquake, a structural system performs two kinds of vibrating motion:

— forced vibration during the shock pulses;

— free vibration between pulses.

Since pulses follow at quite irregular intervals, and both the time intervals and the pulse times are infinitesimal, there is little risk of resonance causing material fatigue.

(In some deep-focus earthquakes, the surface wave motion has a frequency as low as to approach the circular eigenfrequency of certain frameworks. Therefore neither the problem of resonance could be omitted, as shown by the ulterior evaluation of the Bucharest earthquake in March 1977.)

Thus, partly because of the omissibility of resonance, and partly of the likely number of vibration cycles in an earthquake, much below that inducing fatigue, the fatigue characteristics of the material need not reckoning with.

Another advantage is the very high speed of deformations — either in forced or in free vibrations.

Let us consider now the resulting modifications of strength characteristics, considered to be favourable.

3.21 Variation of the strength characteristics of the material vs. displacement velocity

Variation of the vibration, displacement velocity due to seismic shocks is quite important, either in forced or in free vibrations.

Building structures of a silicate material have also viscous properties. Thus, it is advisable to take possibilities of stress increase either concomitant to the variation of displacement velocity or peculiar to viscous materials into consideration.

Yield point increase of steel under variable loading velocities is seen in Fig. 4 after [17].

The yield point increase assuming linear and nonlinear variation is seen in Fig. 5.

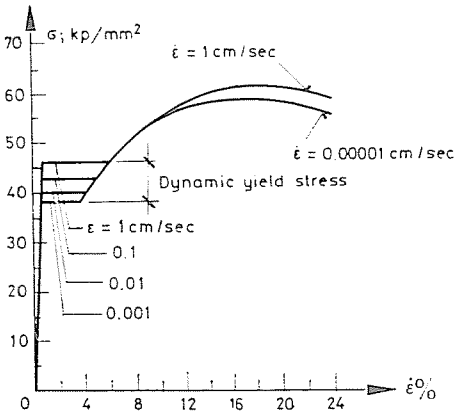

Fig. 4. Effect of strain rate $\dot{\varepsilon}$ on stress-strain curve for structural steel [17]

Linear variation is expressed by [11]:

$$\sigma_f(t) = \sigma_{f0}\left(1 + \frac{\dot{\varepsilon}}{\dot{\gamma}_0}\right) \tag{1}$$

and nonlinear variation:

$$\sigma_f(\ ) = \sigma_{f0}\left[\left(1 + \frac{\quad}{\dot{\varepsilon}_0}\right)^{\frac{1}{n}}\right] \tag{2}$$

where σ_{f0} is yield point for the static condition $\dot{\varepsilon} = 0$; $\sigma_f(t)$ variation of the dynamic yield point; $\dot{\gamma}$, $\dot{\varepsilon}$ and n are test values. In case of steel, e.g., $\dot{\gamma} = 100$ to 300 $\sec^{-1}$; $\dot{\varepsilon}_0 = 40$ $\sec^{-1}$; $n = 5$.

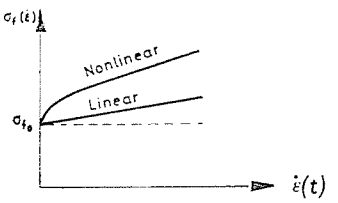

Fig. 5. Yield point vs. strain rate [11]

Concrete as a typically viscous material is rather sensitive to the yield stress increase upon high-speed load effects.

According to [17], by increasing the load rate, ultimate concrete strength may exceed by 80% the ultimate strength under a static load.

Under dynamic effects, also the moduli of elasticity and shear (E, G) may be expected to increase. Design codes specify an increase by about 30% related to the static condition.

Concrete fatigue — to be determined by tests — is, however, a drawback even in case of low-cycle loads, especially in the range of failure.

Load rate to concrete compressive strength relationship is seen in Fig. 6 [17].

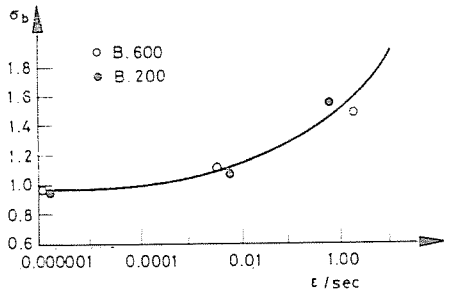

Fig. 6. Compressive strength vs. strain rate [17]

The relationship between strain rate and stress variation is also described by the classic *Prandtl* formula [10]:

$$\sigma_1' = \sigma_0 + \frac{a \cdot A}{A_n} \cdot \ln \frac{C_0}{C_i} \tag{3}$$

where C_0 and C_1 are two different rate values, $\left(\frac{d\varepsilon_0}{dt}, \frac{d\varepsilon_1}{dt}\right)$; σ_0 and σ_1 being the relevant stresses, a is a constant, and A the tested cross section area. Provided $A = A_n$, along the section of uniform strain:

$$\sigma_1 = \sigma_0 + a \ln \frac{C_0}{C_1} . \tag{4}$$

Putting lg instead of ln in (4), for steel $a = 450.00$; for copper $a = 120.00$ and for a light alloy $a = 100.00$ kp/cm^2.

In the free vibration phase between consecutive shocks, also damping is of importance. Evidently, variation of the damping coefficient also depends on the concrete stress state. Relevant tests are being made in the Building Laboratory of the Technical University, Budapest.

Referring to results by JACOBSEN, [17] quotes a damping coefficient $p_c = 0.3$ upon abrupt dynamic effect. This is a rather advantageous maximum compared to $p_c = 0.05-0.25$ generally recommended for viscous materials.

3.22 Specific energy at failure

Although in the following the internal — inherent — work of the structure will be given in terms of the real power-displacement $R-x$ rather than of the specific $\sigma-\varepsilon$, it seems advisable to interpret and write the specific energy at failure in the reference system $\sigma-\varepsilon$ [10].

Specific energy is understood as internal work for unit volume of material:

$$W = \int_{L_0}^{L} \frac{F\,\mathrm{d}l}{V_0} \tag{5}$$

where F is force and v_0 the volume.

Simplified:

$$W = \int_{L_0}^{L} \frac{F\,\mathrm{d}l}{V_0} - \int_{0}^{\varepsilon} \sigma \cdot \mathrm{d}\varepsilon\,. \tag{6}$$

Let us write the specific work at failure interpreted according to a tensile test along three characteristic sections of the $\sigma-\varepsilon$ diagram, Fig. 7.

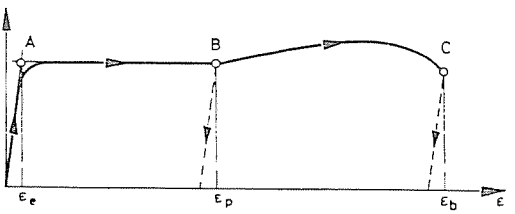

Fig. 7

a) *Elastic range*, assuming *Hooke*'s law to be valid:

$$W_e = E_{\mathrm{pot}\,e} = \int_0^{\sigma_f} \sigma \cdot \mathrm{d}\varepsilon = \int_0^{\sigma_f} \frac{\sigma}{E}\,\mathrm{d}\sigma = \frac{\sigma_f^2}{2E}\,. \tag{7}$$

b) *Plastic range :* assuming as an approximation a constant σ_f value to belong to the deformation between points A—B:

$$W_p = E_{\mathrm{pot}\,p} = \sigma_f \cdot \int_{e_e}^{e_p} \mathrm{d}\varepsilon\,. \tag{8}$$

c) *Contraction work :* assuming the effective stress vs. specific contraction to be about linear in this section,

$$\sigma' = \sigma'_n + \frac{\sigma_m(\psi - \psi_m)}{1 - \psi_m} \tag{9}$$

[10] where ψ and ψ_m are specific and maximum contraction, resp.; and

$$\lambda = \ln \frac{1}{1 - \psi_m} . \tag{10}$$

Contraction work: [10]

$$W_c = E_{\text{pot e}} = \int_{\lambda_m}^{\lambda} \sigma' \, \mathrm{d}\lambda = \int_{\lambda_m}^{\lambda} (2\sigma'_m + \sigma'_m \cdot e^{m-\lambda}) \, \mathrm{d}\lambda = [2\sigma'_m(\lambda - \lambda_m \cdot e^{\lambda_m - \lambda})]_{\lambda m}^{\lambda} =$$

$$= 2\sigma'_m(\lambda - \lambda_m) - \sigma_m(1 - e^{\lambda_m - \lambda}). \tag{11}$$

Substituting λ according to (10):

$$W_c = E_{\text{pot}} = 2\sigma'_m \ln \frac{1 - \psi_m}{1 - \psi} - \sigma'_m \frac{\psi - \psi_m}{1 - \psi_m} . \tag{12}$$

Total strain work in tension or potential energy:

$$W = W_e + W_p + W_c .$$

The mechanism of rupture or failure confirms that the value of internal work in the plastic and contraction ranges of materials with plastic properties is higher by an order than the work in the elastic range.

Utilization of this phenomenon in actual structures still awaits to be solved.

Again from the aspect of earthquakes, obviously an important plastic deformation is expected but such a test would be at most informative beyond the contraction limit.

The degree how to take the work done in the plastic range into consideration in real conditions on effective structures depends — among others — on:

— Whether the structural material has an adequate ductility. The ductility coefficient of steel is known to be about $\eta_{\text{duct}} = \frac{x_{p\max}}{x_{e\max}} \sim 6-8$ but for reinforced concrete is is as low as 3 to 4.

— Whether such important plastic deformations may be permitted at all in a real structure without risking the overall loss of stability. Namely this risk makes the important deformability useless.

Thus, in ultimate analysis, knowledge of the ductility of structural materials is of importance, just as of the plastic deformations likely to raise stability problems.

Remind perhaps that in a structural system the plastic hinges can be located according to principles such that partly to about optimize the inner deformational work of the structure, and partly to have a plastic yield mechanism at no stability loss upon the encountered important deformations.

4. Analysis of a single-mass system of one degree of freedom

4.1 Elasto-plastic range

The single-mass model of one degree of freedom in Fig. 8 simulates a real structural system provided identity between dynamic characteristics is granted.

The model — as a substituting system — is assumed

- to be of an elasto-plastic material;
- plastic deformation much exceeds the elastic one, hence
- in the elastic range, resistance of the system $R(x) = k \cdot x$ is the function of displacement where k is the spring stiffness, x the elastic displacement value;
- in the plastic range, resistance R_0 is independent of the displacement value;
- the system is assumed to be acted upon in the plane of restraint by an initial displacement x_0 of acceleration $\bar{a}_0$ simulating a single shock, causing the centroid m to perform an effective displacement $x(t)$ and the structure a relative one $x_{rel} = x - x_0$.
- Analysis of the elastic range assumes $x_{rel} \leq x_{e\,max}$ and of the plastic range $x_{rel} \leq x_{p\,max}$.

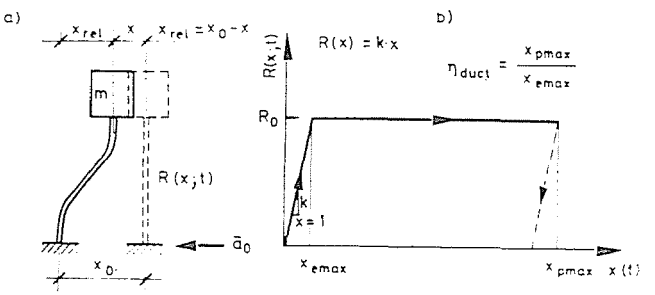

Fig. 8. a) One-degree-of-freedom model; b) Displacement-resistance diagram

Differential equation of motion:

$$m(\ddot{x} - \ddot{x}_0) + k\,x = 0\,. \tag{13}$$

Conditions:

x_0 is an assumed value; $x_{rel} = x_{e\,max}$

$$m \cdot \ddot{x} + k \cdot x = m \cdot \ddot{x}_0 \tag{14}$$

$m \cdot x$ being an assumed or known value. Eq. (14) is mathematically similar to $m\ddot{x} - kx = P(t)$ where again $P(t)$ is an external load of known value. Therefore in the following — for the sake of simplicity — an external load $P(t)$ will be applied, and assuming the known mass, acceleration a will be determined according to the principle of *D'Alembert* and the relevant seismicity according to the MSK scale.

According to Fig. 9 the system is acted upon by an external momentum $P(t) = P_{0f}(t)$.

Load $P(t)$ involves the following assumptions:

— Momentum time t_0 is very short: $t_0 \ll T_0$. T_0 being the eigenfrequency of the system. Thereby a pure momentum load can be spoken of.

— Load function $f(t)$ is perfectly arbitrary and may even change the sign.

— Analysis will refer to the general and special momentum load types a), b), c) and d) in Fig. 10.

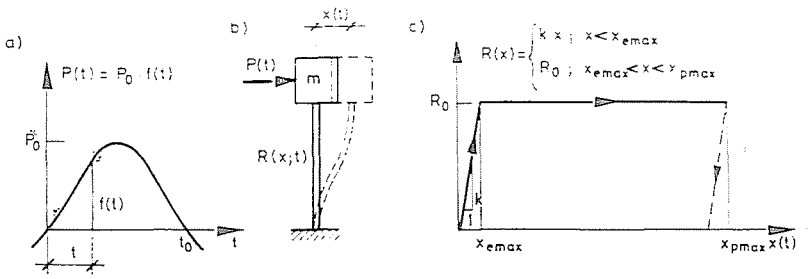

Fig. 9. a) Load-function-momentum diagram; b) Structural model; c) Deformation-resistance diagram

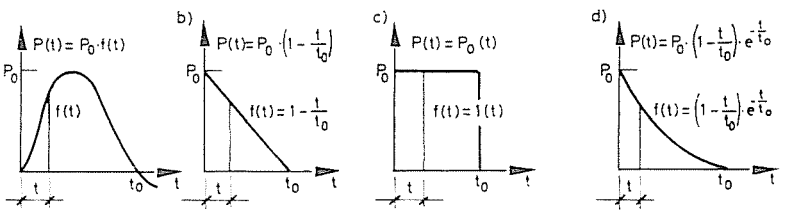

Fig. 10. a) General momentum diagram $I_0 = \int_0^{t_0} p(t)\,dt = P_0 \int_0^{t_0} f(t)\,dt$; b) Triangular momentum-load diagram $I_0 = P_0 \int_0^{t_0} f(t)\,dt = \frac{P_0 t_0}{2}$; c) Rectangular momentum-load diagram $I_0 = P_0 \int_0^{t_0} dt = P_0 t_0$; d) Exponential momentum-load diagram $I_0 = P_0 \int_0^{t_0} \left(1 - \frac{t}{t_0}\right) e^{-\frac{t}{t_0}} = 0.368\ P_0 t_0$

4.11 Effect of general momentum

Differential equation of motion:

$$m\,\ddot{x} + kx = P(t)\,. \tag{15}$$

The condition $t_0 \to 0$ involves that resistance $k \cdot x$ cannot develop in such a short time; term $k \cdot x$ may be omitted:

$$m\ddot{x} = P(t)\,. \tag{16}$$

Integrating both sides yields the velocity function:

$$m\dot{x}(t) = \int P(t)\,\mathrm{d}t;\; v(t) = \frac{P_0}{m}\int_0^t f(t)\,\mathrm{d}t = \frac{I(t)}{m}\,. \tag{17}$$

Kinetic energy:

$$E_{\mathrm{kin}} = \frac{mv(t)^2}{2} = \frac{m}{2}\left[\frac{I(t)}{m}\right]^2;\; E_{\mathrm{kin\,max}} = \frac{[I(t)]^2}{2m}\,. \tag{18}$$

Potential energy is the internal work of the system, represented by the area under the curve of displacement-resistance function $x(t)-R(x,t)$.

Assuming an elasto-plastic condition according to [19], it can be expressed in the elastic range as:

$$E_{\mathrm{pot\,max}} = \frac{R_e X_{e\,\max}}{2} \tag{19}$$

and in the plastic range as:

$$E_{\mathrm{pot\,max}} = R_0 x_{p\,\max}\left(1 - \frac{1}{2}\frac{x_{e\,\max}}{x_{p\,\max}}\right)\,. \tag{20}$$

According to the principle of energy conservation:

$$E_{\mathrm{kin\,max}} = E_{\mathrm{pot\,max}}\,.$$

Making use of it and substituting $I(t) = P_0 \int_0^{t_0} f(t)dt$ the peak load value P_0 is in the elastic range:

$$P_0 = \left[\frac{m}{\int_0^{t_0} f(t)\,\mathrm{d}t}\,R \cdot x_{e\,\max}\right]^{1/2} \tag{21}$$

and in the elasto-plastic range:

$$P_0 = \left\{ \frac{2m}{\left[\int_0^{t_0} f(t)\,\mathrm{d}t\right]^2} R_0 x_{p\max} \left(1 - \frac{1}{2}\frac{x_{e\max}}{x_{p\max}}\right)\right\}^{1/2}. \tag{22}$$

Considering the quotient $\frac{x_{e\max}}{x_{p\max}}$ in (22) as reciprocal of $\eta_{\text{duct}} = \frac{x_{p\max}}{x_{p\max}}$ and knowing the values of momentum $I(t)$ and of R_0, the rate of the maximum displacement $x_{\max}$ may be determined.

Again, writing the equality of both energies:

$$E_{\text{kin max}} = E_{\text{pot max}} : \quad \frac{I(t)^2}{2m} = R_0 x_{p\max}\left(1 - \frac{1}{2\eta}\right) \tag{23}$$

hence:

$$x_{p\max} = \frac{I(t)^2}{2R_0 m\left(1 - \frac{1}{2\cdot\eta_0}\right)}. \tag{24}$$

For $\eta_0 = 1$, i.e. $x_e = x_p$, there is no plastic strain, from (24) substituting $\eta_0 = 1$, $x_{\max} = 1$, x_e is recovered. With increasing ductility coefficient, also $x_{p\max}$ will go increasing.

This case essentially approximates that of the pure plastic range, x_e being rather small compared to x_p. Substituting $\eta_D = \frac{x_p}{x_e} \to \infty$ yields $\frac{1}{2\eta_D} \to 0$ hence:

$$x_{\max} = x_{p\max} = \frac{[I(t)]^2}{2\,R_0 m} \tag{25}$$

corresponding, according to the principle of equality of energies, to the perfectly plastic range;

$$x_{p\max} R_0 = \frac{[I(t)]^2}{2m}. \tag{26}$$

4.12 Linear load function (Figs 11 and 12)

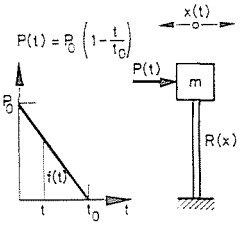

Fig. 11. $I_0 = \frac{P_0 t_0}{2}$: $E_{\text{kin}} = \frac{I(t)^2}{2m} = \frac{P_0^2 \cdot t_0^2}{8m}$

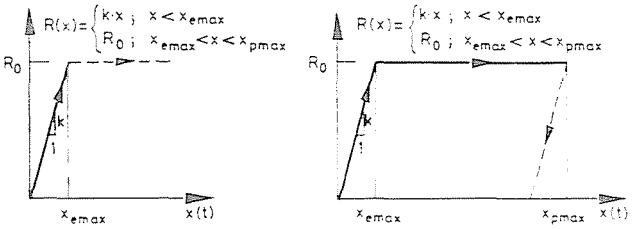

Fig. 12. $x_{\max} = x_{e\max} \rightarrow \eta_{\text{duct}} = 1$: $x_{\max} > x_{e\max} \rightarrow \eta_{\text{duct}} > 1$

Perfectly elastic range: $E_{\text{kin}} = E_{\text{pot}}$ *Elasto-plastic range:*

$$E_{\text{kin}} = \frac{P_0^2 \cdot t_0^2}{8m}; \quad E_{\text{pot}} = \frac{R_0 \cdot x_{e\max}}{2}$$

$$P_0 = \left[\frac{4m}{t_0^2} \cdot R_0 \cdot x_{e\max}\right]^{\frac{1}{2}} \qquad (27)$$

$$x_{\max} = \frac{I_0^2}{2R_0 \cdot m\left(1 - \frac{1}{2\eta_0}\right)} =$$

$$= \frac{\frac{P_0^2 \cdot t_0^2}{4}}{2R_0 \cdot m\left(1 - \frac{1}{2}\right)} = \frac{P_0^2 \cdot t_0^2}{4R_0 \cdot m} \qquad (28)$$

$$E_{\text{kin}} = \frac{P_0^2 \cdot t_0^2}{8m}; \quad E_{\text{pot}} = R_0 \cdot x_{p\max}\left(1 - \frac{1}{2} \cdot \frac{x_e}{x_p}\right)$$

$$P_0 = \left\{\frac{8m}{t_0^2}\left[R_0 \cdot x_p\left(1 - \frac{1}{2}\frac{x_e}{x_p}\right)\right]\right\}^{\frac{1}{2}} \qquad (29)$$

$$x_{\max} = \frac{I_0^2}{2R_0 \cdot m\left(1 - \frac{1}{2\eta_0}\right)} =$$

$$= \frac{\frac{P_0^2 \cdot t_0^2}{4}}{2R_0 \cdot m\left(1 - \frac{1}{2\eta_0}\right)} =$$

$$= \frac{P_0^2 \cdot t_0^2}{8R_0 \cdot m\left(1 - \frac{1}{2\eta_0}\right)} \qquad (30)$$

hence $x_p = x_e$, verified in the item above.

4.13 Constant load function (Fig. 13)

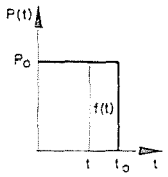

Fig. 13. $I_0 = P_0 \cdot t_0$: $E_{kin} = \frac{I_0^2}{2m} = \frac{P_0^2 t_0^2}{2m}$

Perfectly elastic range: $E_{kin} = E_{pot}$ *Elasto-plastic range:*

$$E_{kin} = \frac{P_0^2 \cdot t_0^2}{2m} ; \quad E_{pot} = \frac{R_0 \cdot x_e}{2} ;$$

$$\frac{P_0^2 \cdot t_0^2}{2} = \frac{R_0 \cdot x_e}{2}$$

$$P_0 = \left(\frac{R_0 \cdot x_e \cdot m}{t}\right)^{\frac{1}{2}} \qquad (31)$$

$$x_{max} = x_e = \frac{P_0^2 \cdot t_0^2}{2R_0 \cdot m\left(1 - \frac{1}{2}\right)} =$$

$$= \frac{P_0^2 \cdot t_0^2}{R_0 \cdot m} . \qquad (32)$$

$$E_{kin} = \frac{P_0^2 \cdot t_0^2}{2m} ;$$

$$E_{pot} = R_0 \cdot x_p \left(1 - \frac{1}{2} \cdot \frac{x_e}{x_p}\right)$$

$$P_0 = \left\{\frac{2m}{t_0^2}\left[R_0 \cdot x_p \left(1 - \frac{1}{2}\frac{x_e}{x_p}\right)\right]\right\}^{\frac{1}{2}} \qquad (33)$$

$$x_{max} = x_p = \frac{I_0^2}{2R_0 \cdot m\left(1 - \frac{1}{2\eta_D}\right)} =$$

$$= \frac{P_0^2 \cdot t_0^2}{2R_0 \cdot m\left(1 - \frac{1}{2\eta_D}\right)} . \qquad (34)$$

4.14 Exponential load function (Fig. 14)

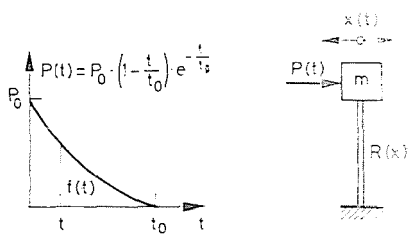

Fig. 14. $I_0 = 0.1354\ P_0^2 \cdot t_0^2$; $E_{kin} = \frac{I_0^2}{2m} = \frac{0.1354\ P_0^2 \cdot t_0^2}{2m}$

Perfectly elastic range: $E_{kin} = E_{pot}$ *Elasto-plastic range:*

$$E_{kin} = \frac{0.1354 \cdot P_0^2 \cdot t_0^2}{2m} \; ; \qquad E_{kin} = \frac{0.1354 \cdot P_0^2 \cdot t_0^2}{2m} \; ;$$

$$E_{pot} = \frac{R_0 \cdot x_e}{2} \qquad E_{pot} = R_0 \cdot x_p \left(1 - \frac{1}{2} \cdot \frac{x_e}{x_p}\right)$$

$$P_0 = \left(\frac{R_0 \cdot x_e \cdot m}{0.1354 \cdot t_0^2}\right)^{\frac{1}{2}} \qquad (35) \qquad P_0 = \left\{\frac{2m}{0.1354 \cdot t_0^2}\left[R_0 \cdot x_p\left(1 - \frac{1}{2} \cdot \frac{x_e}{x_p}\right)\right]\right\}^{\frac{1}{2}}$$

$$x_{max} = \frac{I_0^2}{2R_0 \cdot m\left(1 - \frac{1}{2\eta_D}\right)} \qquad (36) \qquad x_{max} = \frac{I_0^2}{2R_0 \cdot m\left(1 - \frac{1}{2\eta_D}\right)} = \qquad (37)$$

$$= \frac{0.1354 \cdot P_0^2 \cdot t_0^2}{2R_0 \cdot m\left(1 - \frac{1}{2\eta_D}\right)} \qquad (38)$$

4.15 Numerical example

Let us examine the model in Fig. 15 for three kinds of momentum loads (linearly variable, constant, exponentially variable). Assuming perfectly elastic and elasto-plastic ranges, for the given values let us determine the peak load P_0 and the caused displacement x_{max}.

a) *Linearly variable load function*

Perfectly elastic range: *Elasto-plastic range:*

$$P_0 = \left(\frac{4m}{t_0^2} R_0 \cdot x_e\right)^{\frac{1}{2}} =$$

$$= \left(\frac{4 \cdot 100}{0.20^2} \cdot 1000 \cdot 1\right)^{\frac{1}{2}} = \underline{3162.75 \text{ kp}}$$

$$x_{max} = \frac{P_0^2 \cdot t_0^8}{4R_0 \cdot m} = \frac{3162.75^2 \cdot 0.20^2}{4 \cdot 1000 \cdot 100} =$$

$$= \underline{0.9998 \sim 1.00 \text{ cm}}$$

$$P_0 = \left\{\frac{8m}{t_0^2}\left[R_0 \cdot x_p\left(1 - \frac{1}{2}\frac{x_e}{x_p}\right)\right]\right\}^{\frac{1}{2}} =$$

$$= \left\{\frac{8 \cdot 100}{0.20^2}\left[1000 \cdot 10\left(1 - \frac{1}{2} \cdot \frac{1}{10}\right)\right]\right\}^{\frac{1}{2}} =$$

$$= \underline{13784.0487 \text{ kp}}$$

$$x_{max} = \frac{P_0 \cdot t_0^2}{8R_0 \cdot m\left(1 - \frac{1}{2\eta_D}\right)} =$$

$$= \frac{13784.0487^2 \cdot 0.20^2}{8 \cdot 1000 \cdot 100\left(1 - \frac{1}{2 \cdot 10}\right)} =$$

$$= \underline{9.99 \sim 10.00 \text{ cm}}$$

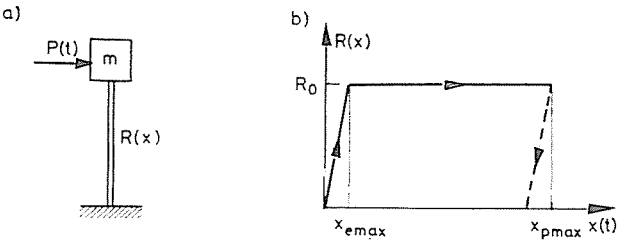

Fig. 15. a) The substitution model; b) Elasto-plastic displacement-resistance diagram: $m = 100.00\ \text{sec}^{-2}\ \text{cm}^{-1}$; $R_0 = 1000.00$ kp; $x_e = 1.00$ $x_p = 10.00$ $\eta_{\text{duct}} = 10.00$; $t_0 = 0.20$ sec; $P_0 = I_0$; $x_{\max} = I_0$

Remark: Reducing the $x_{\max}$ values yields the assumed coefficient

$$\eta_D = \frac{x_p}{x_e} = \frac{9.9998}{0.9998} \simeq 10.00$$

while the plastic reserve can be computed from the direction of peak load P_0 for the plastic and elastic ultimate conditions:

$$k_p = \frac{13784.0487}{3162.75} = 4.3589.$$

Reducing the coefficient of ductility from 10 to 5 yields $\eta_0 = 5$. Omitting calculations, the ratio of peak load P_0 in the plastic ultimate condition: $\frac{9486.8329}{13784.0487} = 0.6882$ and the plastic reserve: $k_p = \frac{9486.0688}{3162.75} = 2.9993$.

b) *Constant load function*

Perfectly elastic range:

$$P_0 = \left(\frac{m}{t_0^2} \cdot R_0 \cdot x_e\right)^{\frac{1}{2}} =$$

$$= \left(\frac{100}{0.20^2} \cdot 1000 \cdot 1\right)^{\frac{1}{2}} = \underline{1581.00 \text{ kp}}$$

$$x_{\max} = \frac{P_0^2 \cdot t_0^2}{2R_0 \cdot m\left(1 - \frac{1}{2\eta_D}\right)} =$$

$$= \frac{1581.00 \cdot 0.20^2}{2 \cdot 1000 \cdot 100\left(1 - \frac{1}{2}\right)} =$$

$$= \underline{0.99 \simeq 1.00 \text{ cm}}$$

Elasto-plastic range:

$$P_0 = \left\{\frac{2m}{t_0^2}\left[R_0 \cdot x_p\left(1 - \frac{1}{2} \cdot \frac{x_e}{x_p}\right)\right]\right\}^{\frac{1}{2}} =$$

$$= \left\{\frac{2 \cdot 100}{0.20^2}\left[1000 \cdot 10\left(1 - \frac{1}{2} \cdot \frac{1}{10}\right)\right]\right\}^{\frac{1}{2}} =$$

$$= \underline{6892.0243 \text{ kp}}$$

$$x_{\max} = \frac{P_0^2 \cdot t_0^2}{2R_0 \cdot m\left(1 - \frac{1}{2\eta_D}\right)} =$$

$$= \frac{6892.0243^2 \cdot 0.20^2}{2 \cdot 1000 \cdot 100\left(1 - \frac{1}{2 \cdot 10}\right)} =$$

$$= \underline{9.99 \simeq 10.00 \text{ cm}}$$

c) *Exponential load function*

$$P_0 = \left(\frac{m}{0.1354 \cdot t_0^2} \cdot R_0 \cdot x_c\right)^{\frac{1}{2}} =$$

$$= \left(\frac{100}{0.1354 \cdot 0.20^2} \cdot 1000 \cdot 1\right)^{\frac{1}{2}} =$$

$$= \underline{4296.95 \text{ kp}}$$

$$x_{\max} = \frac{0.1354 \cdot 0.2^2 \cdot 4296.95^2}{2 \cdot 1000 \cdot 100\left(1 - \frac{1}{2}\right)} =$$

$$= \underline{0.99 \simeq 100 \text{ cm}}$$

$$P_0 = \left\{\frac{2m}{0.1354 \cdot t_0^2}\left[R_0 \cdot x_p\left(1 - \frac{1}{2} \cdot \frac{x_e}{x_p}\right)\right]\right\}^{\frac{1}{2}}$$

$$= \left\{\frac{2 \cdot 100}{0.1354 \cdot 020^2}\left[1000 \cdot 10 \times\right.\right.$$

$$\left.\left. \times \left(1 - \frac{1}{2}\frac{1}{10}\right)\right]\right\}^{\frac{1}{2}} = \underline{18729.98 \text{ kp}}$$

$$x_{\max} = \frac{0.1354 \cdot 18729.98 \cdot 0.20^2}{2 \cdot 1000 \cdot 100\left(1 - \frac{1}{2 \cdot 10}\right)} =$$

$$= \underline{9.99 \simeq 10.00 \text{ cm}}$$

Comments on the results. For any three momentum functions, the peak load value P_0 essentially depends on the peak resistance R_0 and the coefficient $\eta_D = \frac{x_p}{x_e}$. Resistance R_0 is indispensable not only from the aspect of seismic effects but also for wind loads and other lateral effects, hence it is provided in most well designed constructions as lateral stiffness. It is rather costly to increase, besides of being rather inconvenient against seismic effects. The stiffer the structure, the higher the dynamic factor.

Its seems better to increase the coefficient of ductility as a measure against seismic effects.

These examples involved $\eta_D = 10$, rather difficult to achieve for r.c. structures. In this case the plastic reserve, i.e. quotient $k_r = \frac{P_{0p}}{P_{0r}}$ is about 4.389.

Reducing the value of coefficient η_D from 10 to 5 and maintaining R_0 yields the following conclusions, omitting calculations:

— Obviously, peak load P_{0e} belonging to the elastic limit condition is invariable.
— The P_{0p} value belonging to the plastic limit will be 0.6882 times that calculated from $\eta_D = 10$.
— The plastic reserve decreases from 4.389 to 3.00.

These results support the possibility to conveniently and efficiently increase the ultimate plastic resistance to seismic effects of constructions duly designed for wind loads and other lateral effects and possessing an adequate horizontal stiffness, by increasing the ductility, without further increasing the actual stiffness.

The previous results refer to an external shock load. As mentioned in item *4.1*, to simplify calculations, seismic force S_0 due to acceleration $\bar{a}_0$ and initial displacement $\bar{x}_0$ are substituted by an external force $P_0 f(t)$ permitted by the mathematical similarity of Eq. (14).

Below, the seismic acceleration for peak load P_0 will be determined in the MSK scale.

Equality between external load P_0 and seismic force S_0 ($P_0 = S_0$) is started from.

If mass m and mass force S_0 are known, according to the *D'Alembert* principle:

$$m \cdot \bar{a}_0 - S = 0 \,. \tag{39}$$

Hence:

$$\bar{a}_0 = \frac{S_0}{m} \,. \tag{40}$$

Mean accelerations according to the MSK scale are recapitulated in Table 1, permitting to determine the seismic force grade for $P_0 = S_0$.

Table I

MSK scale

Grade	Average surface acceleration $\bar{a}_0$ [cm sec^{-2}]
VI.	5.00—10.00
VII.	10.00—25.00
VIII.	25.00—50.00
IX.	50.00—100.00

Let us consider, e.g. the seismic forces for the elastic and plastic P_0 belonging to the linear load function:

$$P_{0e} = 3162.75 \text{ kp}; \; \bar{a}_0 = \frac{S_0}{m} = \frac{3162.75}{100} = 31.6275 \text{ cm sec}^{-2} \rightarrow \text{VIII MSK}$$

$$P_{0p} = 13784.0487 \text{ kp}; \; a_0 = \frac{S_0}{m} = \frac{13784.0487}{100} = 137.84 \text{ cm sec}^{-2} \rightarrow \text{IX MSK}.$$

Accordingly, the structure with the indicated characteristics could support an earthquake MSK grade a_0 IX to the expense of large plastic deformations. This is still inadequate to predict whether the structure will collapse or not. Namely also the stability questions for very large deformations have to be solved, belonging to the scope of real structures.

4.2 *Analysis of the pure plastic condition*

Utilizing [11], cases of negligible elastic deformation compared to the plastic one will be considered.

Again, a single-mass system with one degree of freedom will be examined under the previously considered three momentum loads (Fig. 16).

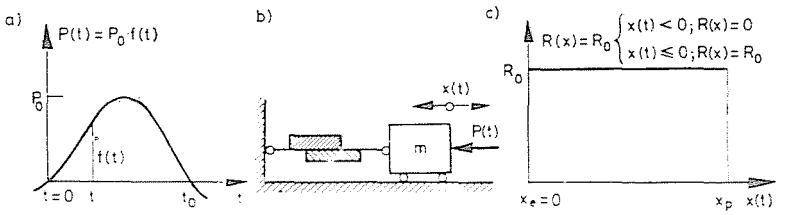

Fig. 16. a) Momentum load diagram; b) Plastic model; c) Plastic displacement-resistance diagram

Starting assumptions are:

— peak resistance R_0 is independent of the displacement:

$$R(x) = R_0$$

— there is no displacement for $P_0 < R_0$;

— arbitrary displacement is possible for $P_0 = R_0$;

— the system is unfit for supporting a force $P_0 > R_0$.

Let us determine the motion time t_{max} and the displacement x_{max} due to an external shock load.

Formerly, the theorem of equality of energies has been applied for determining the unknowns. The actual expressions are, however, much easier to handle by directly integrating the differential equations, taking the definable initial conditions into consideration.

The differential equation of motion:

$$m\,\ddot{x}(t) = P(t) - R_0\,. \tag{41}$$

According to the initial condition: $t = 0 \rightarrow x(t) = 0$

$$v(t) = \dot{x}(t) = \frac{1}{m}\int_0^t P(t)\,\mathrm{d}t - R_0 t\,. \tag{42}$$

Substituting the equally true conditions $t = t_{max}$; $\rightarrow v(t) = 0$

$$0 = \frac{1}{m}\left[\int_0^{t_{max}} P(t)\,\mathrm{d}t\; R_0\, t_{max}\right] \tag{43}$$

yielding for maximum time of displacement t_{max}:

$$t_{max} = \frac{\int_0^{t_{max}} P(t)\,\mathrm{d}t}{R_0} = \frac{P_0}{R_0}\int_0^{t_{max}} f(t)\,\mathrm{d}t\,. \tag{44}$$

Further integrating Eq. (42) and substituting the initial conditions yields the maximum displacement value:

$$x(t) = \frac{1}{m}\int_0^t \left[\int_0^t p(t)\,\mathrm{d}t - R_0 t\right]\mathrm{d}t\,. \tag{45}$$

Substituting the pair of values $t = t_{max}$: $x = x_{max}$ yields for the maximum displacement of the system:

$$x_{max} = \frac{1}{m}\int_0^{t_{max}} \left[P_0\int_0^{t_{max}} f(t)\,\mathrm{d}t - R_0 t_{max}\right]\mathrm{d}t\,. \tag{46}$$

To the analogy of the model with elasto-plastic properties in the previous item, values belonging to the discussed three types of shock loads will be determined.

— Linear load function:

$$t_{max} = \frac{P_0}{R_0}\int_0^{t_0} f(t)\,\mathrm{d}t = \frac{P_0}{R_0}\int_0^{t_0}\left(1 - \frac{t}{t_0}\right)\mathrm{d}t = \frac{P_0}{R_0}\frac{t_0}{2} \tag{47}$$

$$x_{max} = \frac{1}{m}\int_0^{t_0}\left[P_0\int_0^{t_0} f(t)\,\mathrm{d}t - R_0 t_0\right]\mathrm{d}t = \frac{P_0\,t_0^2}{2m}\frac{t_0}{3} - \frac{R_0}{P_0}. \tag{48}$$

— Constant load function:

$$t_{max} = \frac{P_0}{R_0}\int_0^{t_0}\mathrm{d}t = \left[\frac{P_0}{R_0}\cdot t_0\right], \tag{49}$$

$$x_{max} = \frac{P_0\,t_0^2}{2m}\left[\frac{R_0}{P_0} - 1\right]\,. \tag{50}$$

— Exponential load function:

$$t_{\max} = t_0 \ln \frac{P_0}{R_0} \tag{51}$$

$$x_{\max} = \frac{P_0 t_0}{m}\left[1 - \frac{R_0}{P_0}\left(1 + \ln \frac{P_0}{R_0}\right) + \frac{1}{2} \cdot \ln^2 \frac{P_0}{R_0}\right] . \tag{52}$$

Provided $x_{\max} = x_p$ can be considered as known, peak load P_0 is not difficult to determine either.

It is, however, somewhat more complicated in case of a perfectly plastic model.

4.3 Examination of a bar-like, single-mass system with one degree of freedom

Let us consider bar in Fig. 17 of constant cross section and height H, acted upon at the top by a shock load $P(t)$.

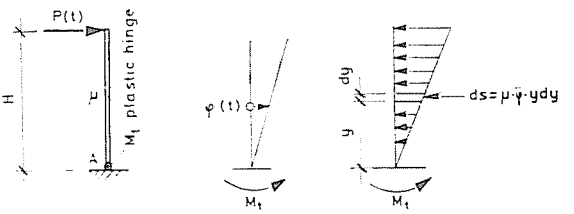

Fig. 17

Initial assumptions:

— The bar has a constant cross section and uniform mass distribution. Specific mass distribution μ = constant.
— It joins the solid medium at point A by a plastic hinge M_t.
— Rotation is only at point A. Other parts of the bar are perfectly rigid during motion, hence exempt of deformation.

Equilibrium equations:

$$\Sigma M_A = 0; \quad P(t) \cdot H - \omega \ddot{\varphi} \frac{H^3}{3} - M_t = 0 \tag{53}$$

$$\omega \ddot{\varphi} \frac{H^3}{3} = P(t)\, H - M_t . \tag{54}$$

Introducing notations and relationships:

$$P_t = \frac{M_t}{H}; \quad p = \frac{P}{P_t} = \frac{P \cdot H}{M} \quad \text{and} \quad p_0 = \frac{P_0}{P_t} = \frac{P_0 H}{M}; \quad \text{for } p_0 < 1, \; x(t) = 0.$$

M_t = ultimate moment at A (plastic hinge);
P_t = ultimate load for M_t;
P = an external load value;
P_0 = external peak load.
Using these notations, Eq. (54) becomes:

$$\omega\ddot{\varphi}\frac{H^3}{3M_t} = p - 1 . \tag{55}$$

Initial conditions:

$$t = 0 \rightarrow \dot{\varphi} = 0$$

$$\mu\dot{\varphi}\frac{H^3}{3M_t} = \int_0^t p\,\mathrm{d}t - t = I(t) - t . \tag{56}$$

After a time $t_{\max}$, displacement is off and the bar is at dead point again:

$$t = t_{\max} \rightarrow \dot{\varphi} = 0$$

$$0 = \int_0^{t_{\max}} p\,\mathrm{d}t - t_{\max};\ t_{\max} = \int_0^{t_{\max}} p\,\mathrm{d}t = I(t_{\max}). \tag{57}$$

For a shock momentum of constant load distribution:

$$I(t_{\max}) = P_0 \cdot t_0 = \frac{P_0}{P_t} \cdot t_0 ,$$

hence:

$$t_{\max} = I(t_{\max}) = \frac{P_0}{P_t} t_0. \tag{58}$$

Utilizing initial condition $t = 0 \rightarrow \varphi(t) = 0$, Eq. (56) yields:

$$\mu\varphi\frac{H^3}{3M_t} = \int_0^t I(t)\,\mathrm{d}t - \frac{t^2}{2} \tag{59}$$

and for $t = t_{\max}$ and $\varphi = \varphi_{\max}$:

$$\mu \cdot \varphi_{\max}\frac{H^3}{3M_t} = \int_0^{t_{\max}} I(t)\,\mathrm{d}t - \frac{t_{\max}^2}{2} . \tag{60}$$

In case of a shock momentum of constant load distribution as simplest case, making use of (58) and of $x_{max} = \varphi_{max} \cdot H$:

$$x_{max} = \frac{3}{4} \frac{P_0 t_0^2}{\mu \cdot H} \left(\frac{P_0}{P_t} - 1 \right) . \tag{61}$$

5. Analysis of real bar structures and structural members

Problems emerged in this study raise two important questions:

a) In a real structure — in particular, in a bar structure — where should plastic hinges develop, partly to keep the system its stable configuration, and partly to have the possible maximum of the inner deformation work — potential energy — of the structure at its ultimate condition?

b) How to design plastic hinges of load capacity $|M_t| = \pm M_t$ — primarily in r.c. structures — likely to cope with the repetitive and alternating flexural stresses due to seismic effects besides of having an important ductility coefficient — higher than the actual one?

The first question will be approached in this chapter, and the second in the next one.

This overall problem is, however, too complicate to be solved within the scope of this paper where neither the analysis according to the second-order theory, nor the multistorey frameworks will be considered.

5.1 Bars

5.11 Bars of continuous mass distribution

Bars of constant cross section and mass distribution, joining the soil by a plastic hinge of load capacity M_t according to Fig. 17 have been considered in item *4.3*. An external shock load $P(t)$ has been assumed and the produced displacement and displacement time values x_{max} and t_{max} sought for.

Now, the same bar will be considered as exposed to a seismic shock of initial acceleration — displacement momentum — $\bar{a}_0$.

Initial assumptions:

— The bar is considered as a perfectly rigid body, suffering only a rotation φ at point A. φ is supposed to be slight and can be discussed by methods valid for small displacements.

— Plastic hinge M_t provides a perfectly plastic connection between bar end and soil $|M_t| = \pm M_t$ (Fig. 18).

Analysis by the Ist-order theory:

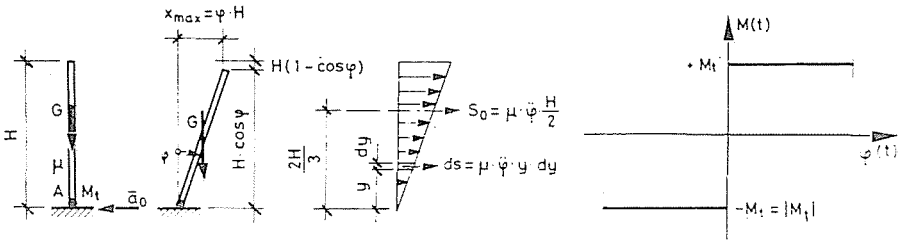

Fig. 18

φ is assumed to be slight, hence: $H(1-\cos\varphi) \simeq H$ accessible to the analysis according to the Ist-order theory. It has to be pointed out, however, that — especially in the analysis of plastic stability, — no treatment according to the IInd-order theory can be dispensed with, since its neglection is to the detriment, rather than on the side of, safety. This is evidenced by Fig. 19 [11].

To the analogy of the former, let us equalize deformation works:

$$w_e = w_i \,. \tag{62}$$

External work is the resultant of mass forces:

$$w_e = \mu \cdot \ddot{\varphi} \cdot \frac{H^2}{2} \frac{2}{3} \varphi \cdot H = \mu \ddot{\varphi} \cdot \frac{H^3}{3} \varphi \,. \tag{63}$$

Internal deformation work:

$$w_i = M_t \varphi_{\max} \tag{64}$$

$$w_e = w_i;\ \mu \cdot \ddot{\varphi} \frac{H^3}{3} \cdot \varphi = M_t \varphi;\ \ddot{\varphi}_{\max} = \frac{3M_t}{\mu \cdot H^3} \,. \tag{65}$$

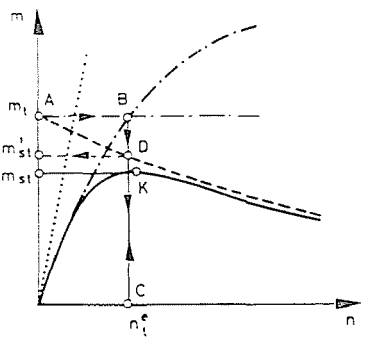

Fig. 19. .... elastic Ist-order; — · — · — elastic IInd-order: — ∘ — ∘ — rigid-plastic Ist-order; ----rigid-plastic IInd order; ——— elasto-plastic IInd-order

This is the greatest circumferential acceleration value possible for a given M_t.

After integrating twice, angular rotation becomes:

$$\varphi(t) = \iint \ddot{\varphi}(t)\,\mathrm{d}t^2 = \iint \frac{3M_t}{\mu \cdot H^3}\,\mathrm{d}t^2 = \frac{3}{2}\,\frac{M_t}{\mu \cdot H^3} \cdot t^2 . \tag{66}$$

Maximum displacement:

$$x_{\max} = \varphi_{\max} \cdot H = \frac{3}{2}\,\frac{M_t}{H^2} \cdot t^2 . \tag{67}$$

Initial conditions:

$$t = 0 \rightarrow \varphi = 0$$

$$t = t_0 \rightarrow \varphi = \varphi_{\max}: \qquad x_{\max} = \frac{3M_t}{2\mu \cdot H^2} \cdot t_0^2 . \tag{68}$$

Maximum mass force value S_0 will be determined from the equilibrium equation $M_A = 0$:

$$\Sigma M_A = 0: \; S_0 \frac{2H}{3} = M_t: \; S_0 = \frac{3M_t}{2H} . \tag{69}$$

As before, ultimate intensity m_t is obtained from the relationship $S_0 = m_t \cdot G$:

$$m_t = \frac{S_0}{G} . \tag{70}$$

Ultimate intensity m_t is the ratio of mass force S_0 — *D'Alembert*'s force — to the total dead weight G in case of a plastic hinge M_t.

5.12 Mass concentrated at the bar end (Fig. 20)

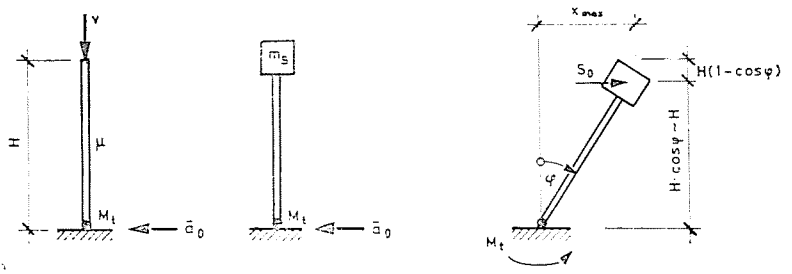

Fig. 20. $m_H = \frac{v}{g} + 0.25\,\mu \cdot H$; $S_0 = m_H \cdot \ddot{\varphi} H = \frac{M_t}{H}$

According to the laws of dynamics, the substituting mass at the bar top:

$$m_s = \frac{v}{g} + 0.25\mu \cdot H :$$

g being the gravity acceleration.

Again, equalizing external and internal work:

$$w_e = w_i ,$$

$$w_e = S_0 x_{\max} = m_s \ddot{\varphi} \cdot H \cdot \varphi = H m_s \ddot{\varphi} H^2 \varphi \tag{71}$$

$$w_i = M_t \varphi_{\max}$$

$$m_H \ddot{\varphi} \cdot H^2 \varphi = M_t \cdot \varphi_{\max} . \tag{72}$$

Maximum angular acceleration:

$$\ddot{\varphi}_{\max} = \frac{M_t}{m_s \cdot H^2} . \tag{73}$$

Function of angular velocity:

$$\omega(t) = \dot{\varphi}(t) = \int_0^t \ddot{\varphi}(t)\, \mathrm{d}t = \frac{M_t}{m_s \cdot H^2} t . \tag{74}$$

Circumferential velocity:

$$v(t) = H \cdot \omega(t) = \frac{M_t}{m_s H} t . \tag{75}$$

Function of angular rotation:

$$\varphi(t) = \int_0^t \dot{\varphi}(t)\, \mathrm{d}t = \frac{M_t}{2 m_s H^2} \cdot t^2 . \tag{76}$$

The displacement for $x(t) = \varphi(t) \cdot H$: (77)

Maximum displacement:

$$x_{\max} = \frac{M_t}{2 m_s H} t_0^2 \tag{78}$$

t_0 being the displacement time.

Ultimate intensity:

$$S_0 = m_t \cdot G ; \; m_t = \frac{S_0}{G} . \tag{79}$$

5.2 *Analysis of a single-storey framework*

Be the single-storey framework in Fig. 21 acted upon by a known force V at mid-span for the sake of simplicity. As before, maximum value of the ultimate intensity $m_t = m_{t\,\max}$, i.e. that failure mechanism is sought for where the plastic deformation work of the structure is maximum.

Initial assumptions:

— Plastic hinges can only develop at nodes and under concentrated loads (points 1 to 5 in Fig. 21). Angular rotations and displacements can only develop in plastic hinges. During motion, other structural parts — bars — behave as perfectly rigid bodies.

— In the analysis of a bar unit, only the flexural moment is taken into consideration.

— The plastic hinge has a moment capacity M_t of identical positive and negative value. Thus, the plasticity condition may be formulated as: $f = M_t - |M| \geq 0$.

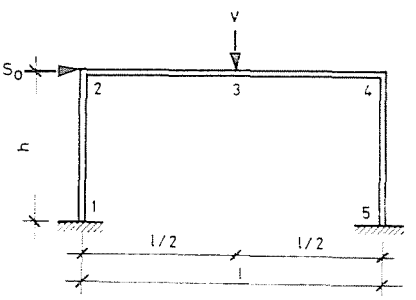

Fig. 21. $S_0 = m_{t\,\max} \cdot V$

— The ultimate moment of plastic hinges is uniform in any cross section of the structure: $M_t = \text{constant}$.

— Vertical load value V is assumed to be constant — value of the dead load of the building and other constant loads to be reckoned with in examining the seismic effect.

— The maximum value of the unknown force H in the ultimate plastic condition of the structure, i.e. the ultimate intensity of force H is sought for. Between V and H there is a one-parameter relation m_t.

The considered structure is a hyperstatic one, with $n = 3$ redundancies. It is known from the theory of strength of materials that a hyperstatic structure with n redundancies is made to a statically determinate, unstable configuration by incorporating $n + 1$ hinges. In our case $n + 1$, at least four plastic hinges have to develop to cause instability.

Failure mechanisms are seen in Fig. 22.

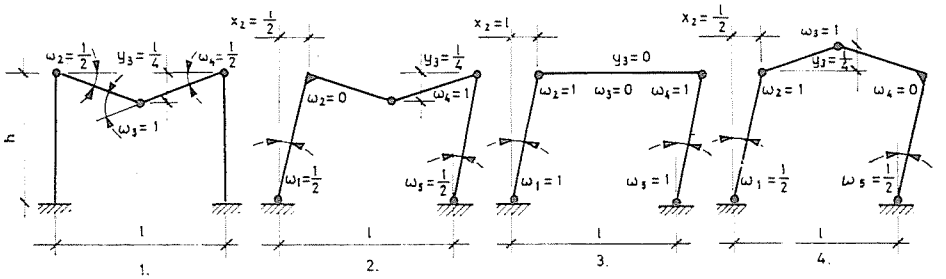

Fig. 22

Displacement and rotation values in the figure are only ratios, permitting to determine the ultimate intensity value. Also here, the analysis is based on

$$w_e = w_i$$

$$w_e = \Sigma V \cdot y_i$$

$$w_i = \Sigma M_i \cdot \omega_i \,.$$

Table II

Symbol of failure mechanism	ω_1	ω_2	ω_3	ω_4	ω_5	$M_t \cdot \Sigma\omega_i$	y_1	y_2	$V \cdot \Sigma y_i$	Ultimate intensity m_t
1	—	$\frac{1}{2}$	1	$\frac{1}{2}$	—	$2M_t$	—	$\frac{l}{4}$	$V \cdot \frac{l}{4}$	$m_t = 0$
2	$\frac{1}{2}$	—	1	1	$\frac{1}{2}$	$3M_t$	$\frac{l}{2}$	$\frac{l}{4}$	$m_t \frac{V}{2} + \frac{V}{4}$	$m_t = \frac{6M_t}{V} - \frac{1}{2} \to m_{t\,\max}$
3	1	1	—	1	1	$4M_t$	l	—	$m_t \cdot V \cdot l$	$m_t = \frac{4M_t}{V \cdot l}$
4	$\frac{1}{2}$	1	1	—	$\frac{1}{2}$	$3M_t$	$\frac{l}{2}$	$-\frac{l}{4}$	$m_t \cdot \frac{V \cdot l}{2} - \frac{V \cdot l}{4}$	$m_t = \frac{6M_t}{V \cdot l} + \frac{1}{2}$

$m_{t\,\max}$, of interest for us, is obtained from mechanism 2. Namely' mechanism 4 could only be produced by a vertical load V if it were due to a wind load $-V$.

Remark that in plastic ultimate analysis, in general, the $m_{t\,\min}$ value is wanted, the failure mechanism where after development of plastic hinges in course of the natural process, the load capacity of the structure is minimum.

On the contrary, our problem consists in finding the failure mechanism concomitant to the maximum ultimate load intensity, and the plastic hinges are designed prealably into the forming mechanism, to ensure development of a possibly propitious failure mechanism. Plastic hinges

of load capacity M_t are designed at spots where their action provides for the optimum ultimate deformation of the structure.

Complex cases, such as multistorey frameworks are outside the scope of this paper.

6. Tests and test results

Question *b)* in Chapter 5 concerned simple plastic hinge units of moment bearing capacity $\pm M_t$, possessing increased ductility and energy absorption under alternating seismic loads. The following three tests were rather promising from this aspect.

Common features of the tests:

— All the three test specimens were exposed to periodic forces inciting displacement: $x(t) = x_0 \sin \cdot \omega t$.

— The maximum displacements were different but the period t_0 was identical in each test.

6.1 *Steel structure model*

No doubt, relevant properties of steel structures or structural units are much superior to those of reinforced concrete.

Thus, the first test was made on a pure steel structural member, assuming that it could also be incorporated in reinforced concrete structures.

The test model of Figs 23, 24, 25, 26 is essentially an elasto-plastic spring unit, where the spring effect is due to the rigidity to displacement of stout steel columns with fixed ends.

Beyond the elastic limit, the columns get in a perfectly plastic state in the clamping plane, hence plastic hinges develop at both ends.

Seismic effects were simulated by applying alternating displacement shocks on the spring units, recording resistances $R(x)$ to the displacement. In the elastic range: $R(x) = k \cdot x$ where k = spring stiffness, and x = elastic displacement.

Beyond the elastic limit — in the plastic range — $R(x) = R_0$, the plastic resistance for the plastic hinge M_t .

The test aimed at determining the number of repetitions of such important plastic deformations the spring unit can endure to still possess any resistance. In other words: the energy-absorptivity of the structure after great plastic deformations.

A similar test method is the accelerated fatigue test (PROT; LOCATI method [10]) known as low-cycle load method.

The method we applied differed by applying identical but very great plastic displacement amplitudes throughout the load test, at a much lower number of cycles.

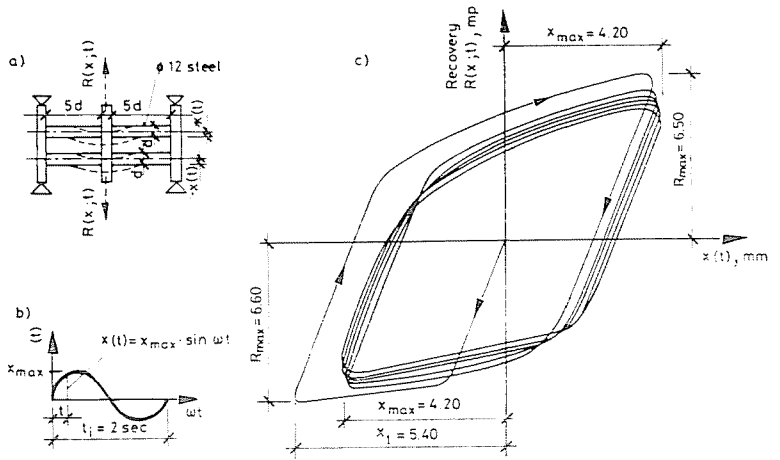

Fig. 23. Model test results. a) Model scheme; b) Displacement momentum; c) Displacement-resistance diagram

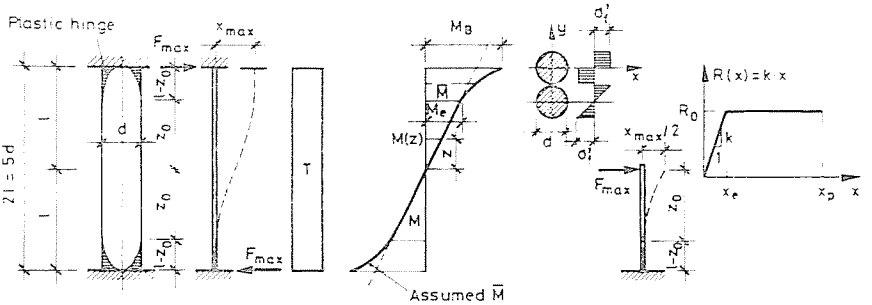

Fig. 24. Deformation of the elasto-plastic bar $M_B = \sigma'_f \cdot K_P$; $K_P = 2S_x$

$$M_e = \sigma'_f \cdot K_e; \quad K_e = \frac{I_x}{y} \quad \overline{M} = \frac{M_e}{\sqrt{3 - 2\,\frac{M(z)}{M_t}}}$$

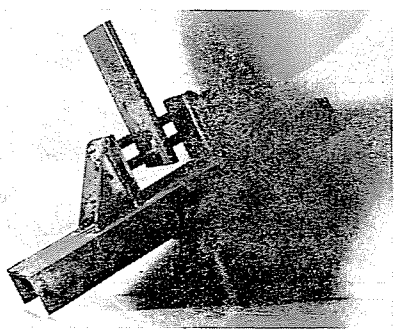

Fig. 25. The spring unit

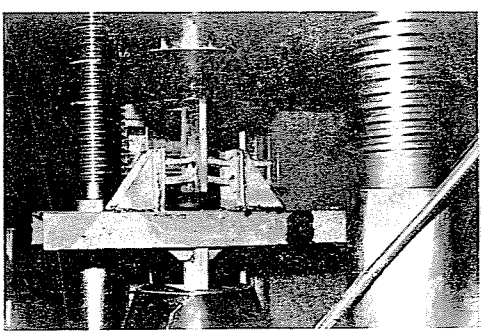

Fig. 26. Spring unit tested

Tests and evaluation:

Models made of high-strength (B.60.40) reinforcing steel have been exposed to the repetitive, alternating effect of 11.50 times the elastic limit of displacement.

After 25 cycles, rigidity to displacement $R(x)$ dropped to a negligible value.

Hence the energy-absorptivity, expressed by the area below the curve $x(t) - R(x;t)$ is rather favourable.

Steels of lower strength but of still higher plastic deformability are likely to behave still better.

Similar steel springs incorporated in real r.c. structures are seen in Fig. 27, together with some application possibilities.

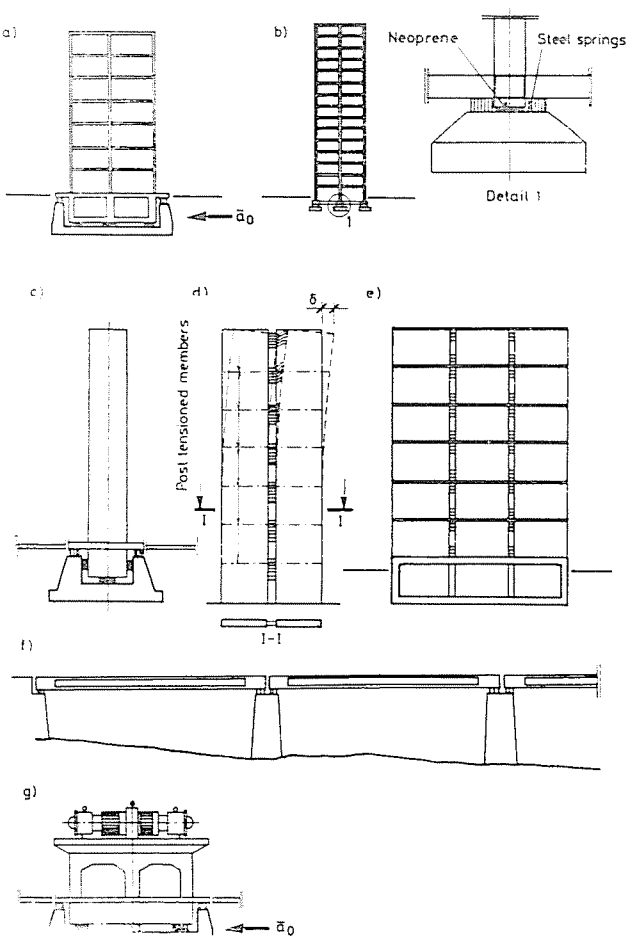

Fig. 27. Practical applications: a) Damping of rigid buildings; b) Solitary foundations; c) Damping of towers; d) Shear wall joints; e) Shear connections of precast wall units; f)Bridges; g) Damping of turbine foundations

In the outlined cases, the steel spring sets act as connections in shear. They are designed to act elastically under constant static loads (e.g. wind, dead load, etc.).

Under seismic effects, large plastic deformabilities may be relied on, maintained even under several repetitions.

Being incorporated into the reinforced concrete so as to work even after this latter cracked and failed, steel springs provide it a much higher ductility and energy-absorptivity. Another field of application is to attenuate propagation of seismic waves to prevent motions from being transferred to the construction.

6.2 Reinforced concrete beams

Comparative test results on a normal r.c. beam and a special one, similar to the former but divided at mid-depth by the described set of steel springs throughout its length will be presented in Figs 28 and 29.

In other words, the latter beam has stirrups absorbing ultimate shear forces but these stand free and are not embedded in concrete.

In great deformations, after the outlined plastic hinges developed, the set of springs unites both r.c. zones and even after important cracking, it is able to resist displacements.

Test results:

6.21 Normal r.c. beam (Fig. 28)

It is a beam of a cross section of 10/25 cm, symmetric reinforcement and ∅ 6/9 cm stirrups, of a span $l_0 = 90$ cm. First, a static deformation had been imposed (Fig. 28a). The elastic limit deformation $x_{e\,\max} = 0.42$ cm.

After the static test, a series of dynamic alternating plastic deformations $x_{p\,\max} = 2.00$ cm have been applied on the beam by means of a pulsating device.

After five cycles, resistance $R(x)$ practically vanished (Fig. 28b).

The value of relative energy absorption is expressed by the area below the curve $x(t) - R(x;t)$ amounting to 3724.00 area units (Fig. 28c).

6.22 Special r.c. beam (Fig. 29)

Its cross section differs from that of the normal beam by ∅ 6 mm steel dowels 5 cm long uniting the two r.c. zones 10/10 cm. The dowels join two steel plates — rather than the concrete — to provide for the rigid clamping of dowels — stout columns — throughout the displacements.

The ultimate moment of this beam was the same as that of the normal r.c. beam.

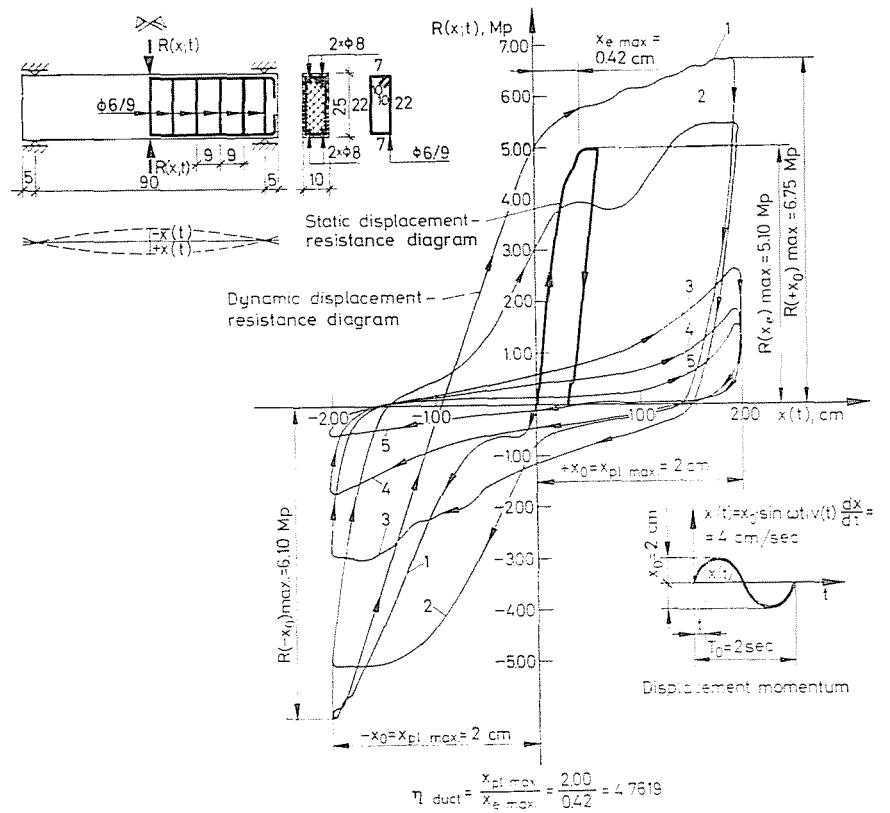

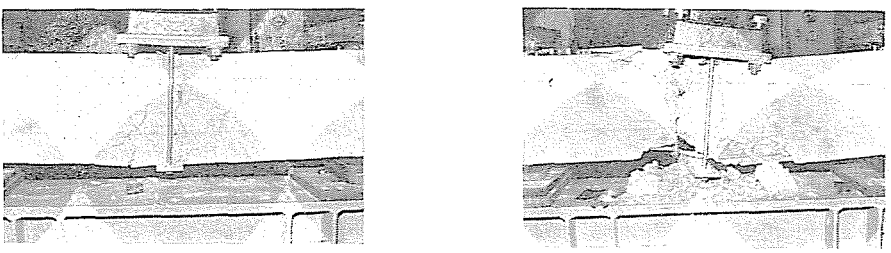

a) *b)*

Fig. 28. Model test on a normal r.c. beam. Concrete grade B 400; steel B 60.40, B 50.36. Relative energy absorption: 40.5 Mp cm; 3724.00 in area units

The elastic limit deformation $x_{e\,\max} = 0.75$. The coefficient of ductility was assumed with about the same value (Fig. 29a).

The imposed maximum plastic deformation $x_{p\,\max} = 3.125$ was endured by the beam q times consecutively, to have its resistance $R(x)$ dropped to a negligible value (Fig. 29b).

The coefficient of energy absorption has been calculated from the nine area units, totalling 7700.00 area units.

Confronted to the normal r.c. beam: $\eta_A = \frac{7700.00}{3724.00} = 2.10$ hence the special r.c. beam of the same ultimate strength and about the same ductility had about twice the energy absorption capacity.

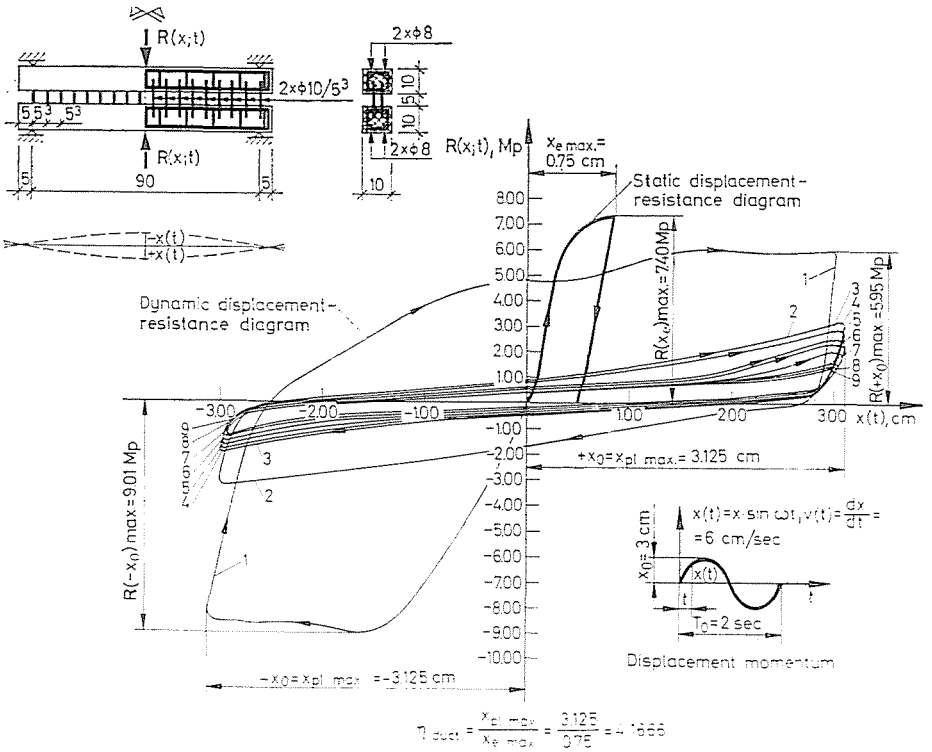

a) *b)*

Fig. 29. Model test on a special r.c. beam. Concrete grade B 400; steel B 60.40. B 50.36; Relative energy absorption: 85.0 Mp cm; 7700.00 in area units; Absorption efficiency:

$$\eta_A = \frac{7700}{3724} = 2.10$$

Summary

This study is meant as an introduction to the research of the complex problem of antiseismic protection.

First of all, comprehensive analysis of the ultimate condition may help in protecting massive constructions of not outstanding importance, hence improper to design for the elastic limit against seismic effects of low probability and of an expected intensity.

Assumption of the ultimate condition may raise debates. It seems, however, still more reasonable than to challenge the fate of great many buildings in an earthquake.

It seems to be better and more economical to anticipate the failure mechanism than to leave it to chance.

Ulterior analysis of failure mechanisms after devastating earthquakes supports the likelihood of averting or diminishing serious fatalities by designing a failure mechanism likely to offset instability and to prevent disjointing.

No adequate number of relevant tests have been made to now to support assumptions but available test results do not contradict them. Even an unambiguous proof is given of the simple and economical possibility to increase ductility.

The subsequent tests on failure mechanisms are expected to support the relevant assumptions.

References

1. Documentations about the influence of the 1963 earthquake on the buildings of Skopje. Report. University of Skopje, Skopje 1966.
2. FALCONER, B. H.: Niigata Earthquake. Report. Tokyo, 1964.
3. ROGERS, P.: The Los Angeles Earthquake. California State University at Los Angeles. 9.02. 1972.
4. LEW, H. S.—LEYENDECKER, E. V.—DICKERS, R. D.: Engineering Aspects of the Los Angeles Earthquake, 1971. Building Science Series 40. Washington D.C. 20234, 1971.
5. Proceedings, FIP International Symposium on Seismic Structures. Tbilissi. 1972.
6. Meeting on Friuli Earthquake. Preprints. Intern. Centre of Mech. Sc. Udine, 4—5, 12. 1976.
7. Contributo allo studio del terremoto del Friuli 1976. CNEN-ENEL Roma, 1976.
8. Il terremoto nel Friuli del Maggio 1976. ANCE, Roma 1976.
9. Il terremoto del 6 Maggio 1976 nel Friuli. L'Industria Italiana de Cemento, Roma, 7—8, 1976.
10. GILLEMOT, L.: Materials and Materials Testing.* University textbook. Budapest, 1967.
11. KALISZKY, S.: Theory of Plasticity.* Akadémiai Kiadó, Budapest, 1976.
12. CSÁK, B.: Inelastic Dynamic Behaviour of Structures under Seismic Loading. IASS Conf. Alma-Ata 1977.
13. PRAGER, W.—HODGE, P. G.: Theory of Perfectly Plastic Solids. John Wiley and Sons, New York.
14. HORNE, M. R.—MERCHANT, W.: The Stability of Frames. Pergamon Press, Oxford, 1965.
15. POLYAKHOV, S.: Design of Earthquake-Resistant Structures. Mir Publishers, Moscow, 1974.
16. KOLLÁR, L.: Stability of Frameworks and Columns.* (BVTV Műszaki Osztály.) Budapest, 1972.
17. NORRIS, C. H.: Structural Design for Dynamic Loads. McGraw Hill, London, 1959.
18. GOSCHY, B.—VÉRTES, GY.: Examination of Structures under Dynamic Effects.* Inst. Post-Grad. Eng. Ed. Budapest, 1964.
19. CIȘMIGIU, A.: The Earthquake of March 4, 1977. (In Rumanian), Architectura (București) 4, 1977.

Dr. Béla CSÁK, H-1521 Budapest

*In Hungarian.